Metal-based nanoparticles dispersed in glycerol: An efficient approach for catalysis

Isabelle Favier, Daniel Pla, Montserrat Gómez

Graphical Abstract

To create your abstract, type over the instructions in the template box below.
Fonts or abstract dimensions should not be changed or altered.

Metal-based nanoparticles dispersed in glycerol: an efficient approach for catalysis

Isabelle Favier, Daniel Pla and Montserrat Gómez*

Leave this area blank for abstract info.

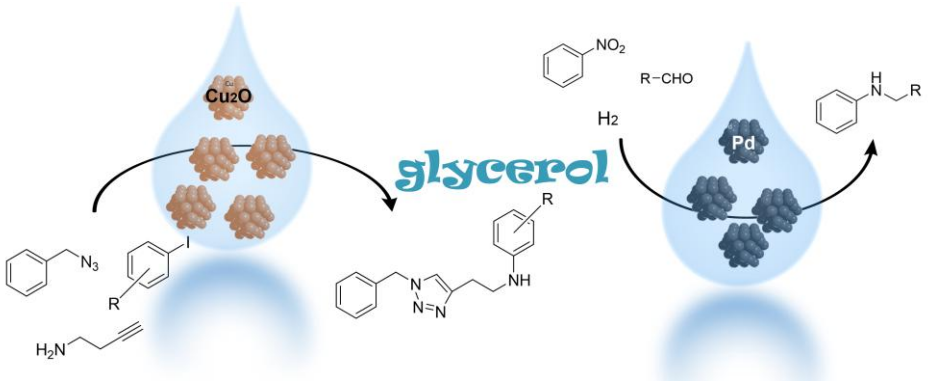

Catalysis Today
journal homepage: www.elsevier.com

Metal-based nanoparticles dispersed in glycerol: an efficient approach for catalysis

Isabelle Favier[a], Daniel Pla[a] and Montserrat Gómez[a,*]

[a] *Laboratoire Hétérochimie Fondamentale et Appliquée (LHFA), Université de Toulouse, UPS and CNRS UMR 5069, 118, route de Narbonne, 31062 Toulouse cedex 9, France.*

ARTICLE INFO

Article history:
Received
Received in revised form
Accepted
Available online

Keywords:
Glycerol
Metal nanoparticles
Metal oxide nanoparticles
Transition metals
Catalysis
Synthesis
Recycling

ABSTRACT

The present mini-review describes the use of glycerol as solvent for the synthesis of metal and metal oxide nanoparticles exhibiting catalytic properties. This contribution specially underlines the ability of glycerol to both disperse and immobilize metal-based nanoparticles, increasing their lifetime. In other words, glycerol can act as a liquid support for nanocatalysts.

1. Introduction

Glycerol, mainly generated as concomitant product in the production of biodiesel, shows attractive physico-chemical properties to be considered as an eco-friendly solvent for synthesis and catalysis purposes: a large temperature range in liquid state (from 17.8 to 290 °C), a negligible vapor pressure (0.003 mmHg at 50 °C), a high ability to solubilize both organic and inorganic polar compounds, and also its immiscibility with low polar solvents (selected reviews: [1-3]). In addition, its high polarity, long relaxation time, high loss tangent value and high acoustic impedance make it appropriate to be used under microwave and ultrasound irradiation conditions, bypassing its main disadvantage for chemical transformations, i.e. its high viscosity (1.4 Pa.s) [4, 5].

Focusing on metal-based nanoparticles, glycerol, analogously to other polyols (e.g. ethylene glycol or polyethylene glycol), has been applied in polyol synthetic methodologies, where the alcohol acts as both solvent and reducing agent of metal precursors (for selected contributions, see [6-8]), with the consequent formation of glycerol oxidation products. With the aim of circumventing this problem, we have developed the synthesis of metal nanoparticles in glycerol applying a low pressure of dihydrogen (< 3 bar) [9], which avoids glycerol hydrogenolysis and glycerol oxidation side reactions [10]. It is important to underline that the supramolecular structure of glycerol [11], prompted by its three different types of hydrogen bonds, favors both dispersion and trapping of nanoparticles, interesting features for catalysis.

* Corresponding author. Tel.: +33561557738; fax: +33561558204; e-mail: gomez@chimie.ups-tlse.fr

In this mini-review, we highlight the contributions concerning the synthesis and catalytic applications of metal-based nanoparticles in glycerol. Currently, the published works mainly involve transition metals from groups 10 and 11. Thus, we have organized this contribution in three main parts: i) Metal-based nanoparticles from group 10; ii) Metal-based nanoparticles from group 11; and iii) Miscellaneous.

Herein, we draw special attention to the reported works on nanocatalysis involving glycerol as a solvent from 2014 to January 2017, representing an update to previous literature reviews [1-3].

2. Metal-based nanoparticles from group 10

2.1. Nickel

Novel methodologies based on variations of the polyol method have been recently reported for the synthesis of metal nanoparticles (MNPs) providing new bottom-up strategies to gain control on the size and shape of the kinetically stabilized metal phases at the nanometric scale.

In particular, zero-valent NiNPs of 100-1000 nm size could be prepared from nickel nitrate using supercritical water (SCW) as a reaction medium and glycerol as an environmentally friendly reducing agent (in comparison to formic acid or hydrazine, commonly used), at 400 °C and 300 bar by a hydrothermal method [12]. In this work, the glycerol/metal precursor ratio was a crucial parameter for the full reduction of metal salts into Ni(0) and Cu(0) species. However, for low electronegative metals (such as Co, Fe and Mn), glycerol reduced the salts into low-valent metal oxides, acting as an anti-oxidant reagent.

The catalytic activity is highly dependent on the size of the metal nanoparticles. Wang and Liu recently reported the preparation of nanocatalysts based on silica supported Ni nanoparticles where the mean particle size could be efficiently tuned by using different alkanol solvents through a wet impregnation method. In particular, the use of glycerol as delivery conveyer and removable carbon template effectively yielded smaller size and uniform dispersions of metal particles of 6-8 nm [13]. This Ni/SiO_2 catalyst prepared by glycerol impregnation was proven to display higher activity and selectivity towards partial oxidation of CH_4, giving conversions up to 94%, and CO selectivity of 88% due to the higher metal dispersion and more unsaturated surface atoms.

Despite the enhanced reactivity patterns of kinetically stabilized Ni nanoparticles and bimetallic systems in glycerol, the right choice of nanocatalyst in combination with the fine tuning of the reaction conditions is of paramount importance to preclude undesired side-reactions of glycerol itself as a substrate. Otherwise, glycerol dehydration and formation of hydroxyacetone [14], and hydrodeoxygenation [14, 15] have been described. Furthermore, the use of glycerol in alkaline media has been reported towards membrane-less direct liquid fuel cell platforms of high performance energy generation systems for transportation and stationary storage [16, 17].

2.2. Palladium

Recent advances on microwave-assisted synthesis of monometallic palladium nanoparticles have been reported in continuous-flow by employing the polyol methodology in glycerol as both reducing agent and solvent, using poly(*N*-vinyl-2-pyrrolidone) as additive,

under microwave irradiation [18]. Furthermore, an analogous continuous synthesis of bimetallic $Pt_{shell}Pd_{core}$ nanoparticles was carried out, where glycerol acts as a reducing agent [19]. Under microwave conditions, glycerol efficiently converts MW energy into thermal activation, also enhanced by its long relaxation time which is related to the supramolecular arrangement by intermolecular hydrogen bonds [20]. The core-shell structure and the nanoparticle size (6.5 ± 0.6 nm) corresponds to one atom layer thickness of Pt (0.25 nm) encapsulating the Pd core metal as elucidated by high-angle annular dark-field scanning transmission electron microscopy (HAADF-STEM) and EDS elemental mapping.

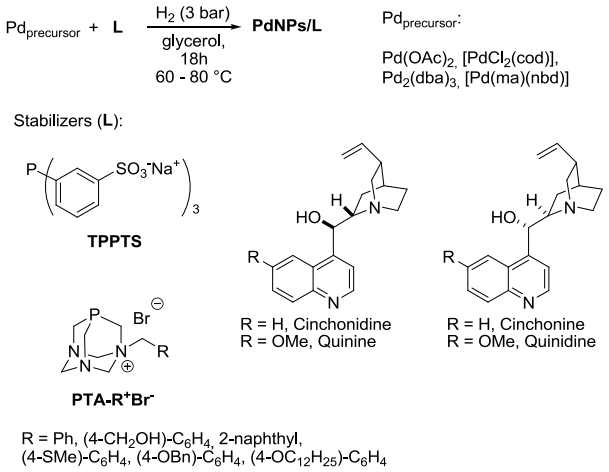

Scheme 1. Synthesis of palladium nanoparticles in glycerol using phosphine and cinchona based ligands as stabilizers.

With the aim of using glycerol merely as solvent, we developed a methodology based on a bottom-up approach for the synthesis of metal and metal oxide nanoparticles. Actually, metal precursors (salts or well-defined organometallic complexes) were decomposed under dihydrogen atmosphere in the presence of stabilizers (for selected contributions, see [21-23]), using glycerol as solvent (Scheme 1). In the absence of any stabilizer other than glycerol, only agglomerates were obtained. The optimization of different parameters such as metal concentration, stabilizer nature, metal/stabilizer ratio, hydrogen pressure and temperature, led to the formation of stable colloidal solutions, which can be stored for several months without loss of catalytic activity. Phosphine and cinchona based ligands gave colloidal solutions constituted by small PdNPs showing a relative narrow size distribution. The nature of the stabilizer induces different surface reactivity, in agreement with the different coordination mode at the metallic surface (Scheme 1).

Following this strategy, Pd nanoparticles were prepared and fully characterized by conventional techniques, both in glycerol solution and in solid state. In particular, the negligible vapor pressure of glycerol enabled TEM and XPS analyses from the colloidal solutions, allowing a direct analysis of the metal-based nanoparticles without isolation at the solid state (Figure 1).

PdNPs stabilized by glycerol-soluble phosphines such as tris(3-sulfophenyl)phosphine trisodium salt (TPPTS) [9, 24, 25] and *N*-substituted 1,3,5-triaza-7-phosphaadamantane ionic ligands (PTA-R^+Br^-) [26], were efficiently applied in different Pd-catalyzed transformations: C-C and C-heteroatom bond formation, hydrogenation and carbonylation, also including multi-step processes for the synthesis of heterocycles [25]. In general, PdNPs stabilized by TPPTS exhibited higher activity than those coming from PTA derivatives. For this reason, here we have chosen to underline the main catalytic achievements of the PdNPs/TPPTS system in glycerol. This colloidal solution was active for different C-C cross-couplings (Suzuki-Miyaura, Heck-Mizoroki and Sonogashira), Michael

conjugate additions using amines, phosphines and thiols as reagents, and hydrogenations of nitro derivatives and a variety of C=C bonds [9]. This versatility led us to apply this system in Pd-catalyzed multi-step processes (e.g. C-C coupling followed by cyclisation; carbonylative couplings followed by cyclization; sequential processes adding a last hydrogenation step) with the aim of synthesizing heterocycles by one-pot/one-catalyst approach (Figure 2). This methodology permitted to obtain the desired products without isolating intermediates. In addition, the catalytic phase was efficiently recycled thanks to the ability of glycerol to immobilize metallic species, giving, in consequence, metal-free isolated organic products.

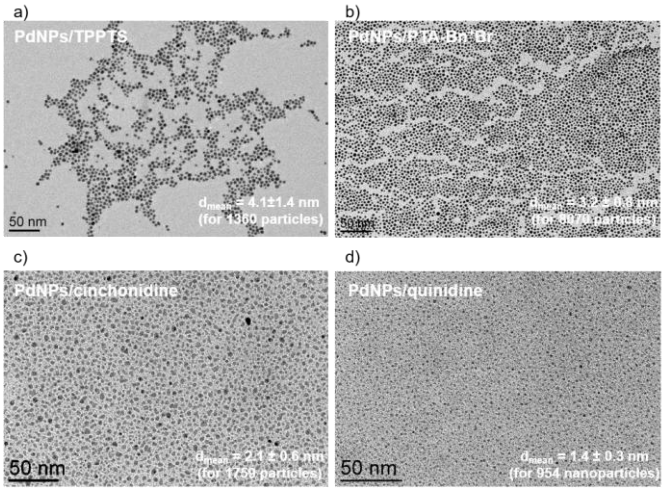

Figure 1. TEM images in glycerol corresponding to PdNPs stabilized by TPPTS (a), PTA-$Bn^{+}Br^{-}$ (b), cinchonidine (c) and quinidine (d). See Scheme 1 for ligand structures [9, 26, 27] .

With the purpose of using stabilizers coming from biomass, we prepared PdNPs in glycerol stabilized by cinchona alkaloids [27]. These ligands, previously used in the literature for the synthesis of supported Pd and Pt nanoparticles [28-31], coordinate to the metal surface through the aromatic quinoline fragment by π-interaction [32-34]. In contrast to phosphines, these ligands disfavor the formation of defined molecular complexes and consequently, privilege the stabilization of metal nanoparticles. Actually, this coordination fact is reflected by their reactivity behavior. While PdNPs stabilized by TPPTS are active for both C-C cross-couplings and hydrogenations, PdNPs containing cinchona ligands (cinchonidine, cinchonine, quinine, quinidine) are efficient catalysts for hydrogenations and hydrodehalogenations under low dihydrogen pressure (Scheme 2a), processes working under surface regime conditions.

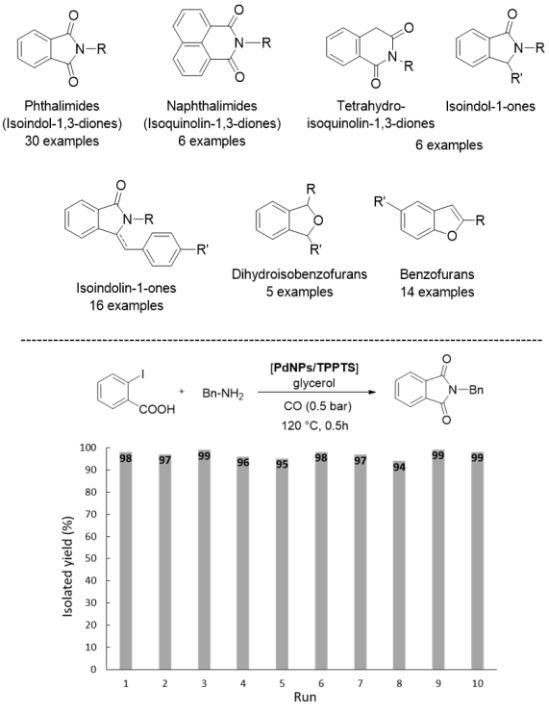

Figure 2. Heterocycles synthesized by Pd-catalyzed multi-step processes in glycerol (using preformed PdNPs stabilized by TPPTS), following a one-pot/one-catalyst methodology (top). Recycling of the catalytic phase illustrated by the phthalimide synthesis (bottom) [25].

PdNPs/quinidine catalytic phase was efficiently applied to the synthesis of amines and *N*-substituted anilines by a one-pot tandem strategy starting from aldehydes and amines or nitrobenzene under H_2 atmosphere, taking advantage of the fact that this catalyst is inactive for the reduction of aldehydes (Scheme 2b).

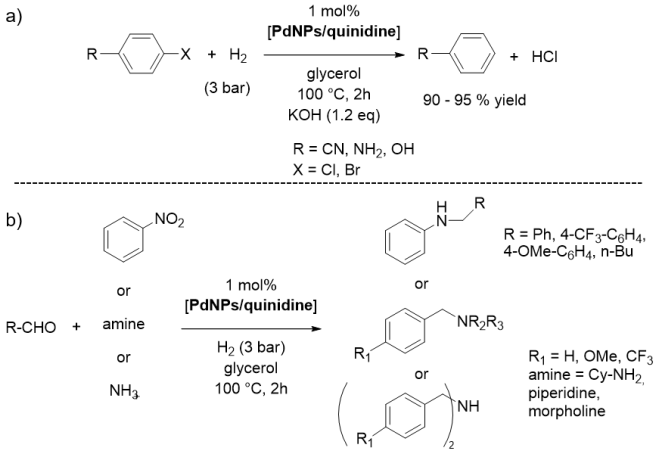

Scheme 2. PdNPs stabilized by quinidine applied in hydrodehalogenations (a) and in the synthesis of amines (b) [27].

Furthermore, the oxidation of glycerol for its potential applications as a portable fuel source and H_2 production have been extensively studied using monometallic palladium nanoparticles [35], and bimetallic combinations thereof (Pd/TiO_2 [36], Pd/ZnO [37], Pd/Ti nanotubes [38], Pd-Ce supported on a metal organic framework Fe-MIL-101-NH_2 [39], Pd-Au/C [40, 41], Pd_{shell}-Au_{core}/C [42], Pd_{shell}-Au_{core}/TiO_2 [43], $PdCu_{alloy}$/*N*-doped multi-walled carbon nanotubes [44]). Besides, the upgrading of glycerol towards the

synthesis of value-added molecules is a research field of raising interest. In particular, recent progress on palladium supported in metal organic frameworks (MOFs) and zeolites shows great potential [45]. These topics fall out of the aims of our present review.

2.3. Platinum

The polyol method for the synthesis of Pt nanoparticles has been upgraded thanks to the efficiency of microwave irradiation in batch [46] and continuous-flow processes [18]. Thus, 2-8 nm spherical-shaped platinum nanoparticles featuring (111) facets were prepared using a Pt(II) precursor salt, glycerol (both as solvent and reducing agent), and polyvinylpyrrolidone (PVP, as stabilizer) under microwave irradiation for 3-5 min at 300 °C [46]. Furthermore, an analogous microwave-assisted methodology for the continuous syntheses of Pd/Pt core-shell nanoparticles through core particle formation coupled with galvanic metal displacement has also been described [19].

The kinetically stabilized colloids prepared by these methodologies showed enhanced electrocatalytic performance towards alkanol transformations [46]. In particular, solvent-controlled platinum nanocrystal growth has rendered up to four tailor-made nano-crystalline structures depending on the growth rates along 〈100〉 to 〈111〉 axis, thanks to the inherent reduction rates of the diverse reaction solutions tested (Fig. 3) [47]. In addition, the branched Pt/C featuring the high-index facet in the edge and stability of facet (111) of the branched nanocrystal exhibits the best electrocatalytic performance due to the highest electrochemically active surface area, enhanced activity of methanol oxidation reaction, together with improved robustness [47].

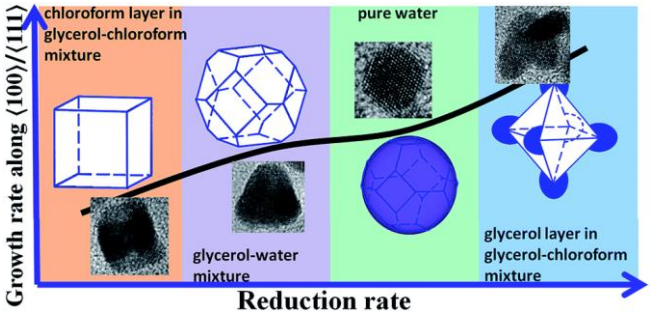

Figure 3. Relationship between the reduction rate and the growth rate along 〈100〉 to 〈111〉 for Pt nanocrystals. Reprinted with permission from reference [47]; license number 4038741241859. Copyright 2017, Royal Society of Chemistry.

3. Metal-based nanoparticles from group 11

Glycerol was used as solvent and reducing agent towards the synthesis of CuNPs by solvothermal reduction method. The reaction was carried out at 150 °C for 40 min starting from $Cu(NO_3)_2$ in the presence of Na_2CO_3 and polyethylene glycol surfactants (PEG200, 6000, 20000) or polysorbate 80 (PS80). Depending on the surfactant nature, the size of the NPs increased from 38 to 50 nm. The authors propose initial formation of Cu_2O and then the reduction to Cu(0) (confirmed by XRD analyses) that could be evidenced by a color

change from blue-green to ocher yellow, and then red-violet. The largest particles were obtained with PEG20000, and the smallest with PS80 [48].

To the best of our knowledge, only few works (out of our contributions) concerning the synthesis of group 11 metal nanoparticles, have been described using neat glycerol as solvent [49, 50]. Ag, Au and Cu nanoparticles were synthesized by laser irradiation, finding that the best way to control the size of MNPs (10-30 nm) was under continuous laser irradiation [49]. An and Zhang prepared hybrid nanoparticles consisting in AgX/Ag nanostructures, i.e. cube-tetrapod-like AgCl/Ag nanoparticles and AgBr/Ag nanoplates. Authors proved that the main role of glycerol in these syntheses was to control the shape of the nano-objects, thanks to its high viscosity at low temperature, controlling the diffusion of ions and consequently diminishing both nucleation and growth rates of AgX [50]. The strong adsorption in the UV-visible spectral region, due to the surface plasmon resonance of the AgX/Ag materials, prompted the authors to apply them as photocatalysts in the reduction of CO_2 to methanol.

The formation of CuNPs was monitored by UV-Vis spectrometry, XANES (X-ray Absorption Near Edge Structure) and TEM in glycerol. Copper-based NPs were prepared from $CuCl_2 \cdot 2H_2O$ dissolved in glycerol at room temperature using hydrazine as reducing agent [51]. XANES analyses indicated that these materials tend to form a mixture of Cu(0) and CuO NPs at a longer reaction times.

Glycerol has been also used as additive for chemical reduction of silver and gold salts in aqueous medium. In particular, glycerol favored the formation of silver nanoplates, inducing a high stability of the as-prepared nano-objects against ripening and oxidation processes, probably due to the reductive nature of the polyol [52]. However, glycerol appears less efficient for the synthesis of gold nanoparticles [53].

Ag, Au and Au@Ag core shell NPs were prepared by dissolving $AgNO_3$ or $HAuCl_4$ salt in aqueous solution with (0-40%vol) glycerol with triethylamine as reducing agent in the presence of PVP or SDS (sodium dodecyl sulfate) as stabilizing agents at room temperature. For the bimetallic system, AuNPs were firstly prepared and after $AgNO_3$ was added with triethylamine and glycerol [54]. The resulting bimetallic NPs showed better antibacterial activity against E. coli than AgNPs.

Ag-based nanofluids were prepared in glycerol in order to study their thermal conductivity and viscosity. Glycerol was chosen for its high heat transfer capacity. The nanofluids were constituted by mesoporous silica or hemiaminal grafted mesoporous silica decorated by AgNPs dispersed in glycerol obtained after ultrasonication. The presence of AgNPs diminishes the viscosity of the mesoporous SiO_2 suspensions due to the diminution of the hydrogen bonds between the silica and glycerol, also increasing the thermal conductivity of the material [55].

In relation to copper, we were interested in the synthesis of Cu_2O nanoparticles by the methodology employed for the synthesis of PdNPs (Scheme 1), starting from $Cu(OAc)_2$ in the presence of polyvinylpyrrolidone as stabilizer [56]. The as-prepared material was fully characterized both in glycerol solution and solid state, confirming the cubic structure of Cu_2O (Figure 4).

Preformed Cu_2ONPs were active in C-heteroatom bond formation, azide-alkyne cycloaddition and one-pot multi-step processes. This catalytic system allowed the synthesis of secondary amines and thioethers by reaction of iodo-aryl derivatives with primary amines or thiols. Furthermore, the synthesis of primary amines could be achieved directly from aqueous ammonia and haloarene substrates,

leading to the corresponding anilines, which were unreactive towards further arylation under these conditions. Products were extracted from the glycerol phase by a biphasic methodology using dichloromethane as extraction solvent, remaining the copper species immobilized in glycerol and in consequence, copper-free organic compounds were directly isolated from the catalytic solution. In contrast to the Cu(I) systems reported in the literature, no co-solvent was necessary to carry out this type of couplings [57, 58].

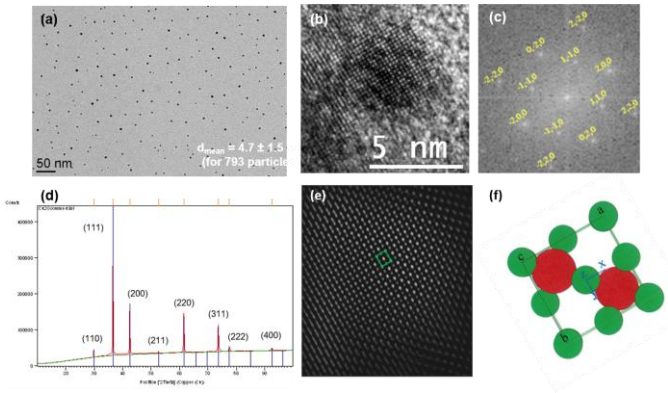

Figure 4. TEM (Ni grid) micrograph of Cu_2ONPs in glycerol (a); HR-TEM micrograph of one isolated particle dispersed in glycerol (b); electronic diffraction spots observed by Fast Fourier Transform of one single particle from image b (c); powder X-ray diffraction analysis of Cu_2ONPs at solid state (d); filtered image showing the zone axis [001] (e), with the corresponding cartoon of the cubic structure of bulk Cu_2O (f). Reprinted with permission from reference [56]; license number 4040820273142. Copyright 2017, John Wiley and Sons.

Since the independent pioneering works from Sharpless [59] and Meldal [60], Cu(I)-based catalytic systems have been largely applied in Cu-catalyzed azide-alkyne cycloadditions (CuAAC) to afford 1,4-triazoles (selected reviews: [61-66]). Cu_2ONPs in glycerol were efficient systems (isolated yields > 90%) for the reaction of benzylazide with different terminal alkynes including alkyl derivatives (Scheme 3a). The glycerol catalytic phase was recycled up to ten times without loss of activity. This robust catalytic system also permits the preparation of unsymmetrically substituted bis(triazoles) by a three-step process, from 1,7-octadiyne and sodium azide followed by sequential addition of benzyl bromide and 4-(methylthio)benzyl bromide.

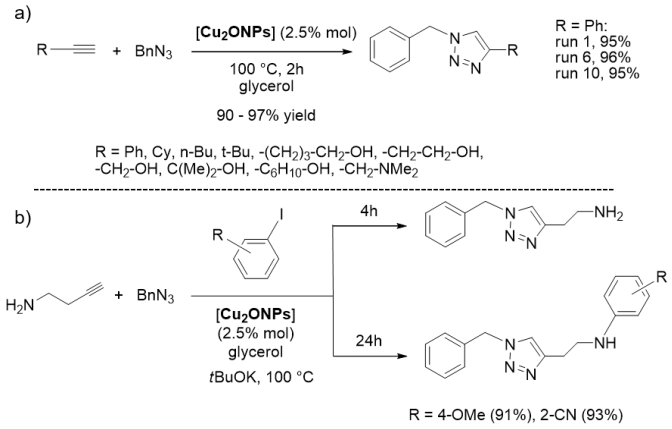

Scheme 3. Cu_2ONPs applied in azide-alkyne cycloaddition (a) and azide-alkyne cycloaddition/C-N coupling tandem processes (b) [56].

We were also interested in using Cu_2ONPs as the only catalyst for tandem processes involving C-N bond formation and AAC for the synthesis of polyfunctional compounds, taking into account that the first process is faster than the triazole formation (monitored by GC). Actually, *N*-substituted anilines containing a triazole moiety were isolated in high yields (Scheme 3b).

With the aim of making easier and pursuing a "click" methodology [67], we studied the CuAAC reaction using CuI in glycerol as catalytic precursor and in the absence of any Lewis base, for the benchmark reaction between phenylacetylene and benzyl azide [68]. Unfortunately, the reaction did not work using the highly pure "home-made" benzyl azide (prepared following the reported protocol [69]). However, when the commercial one was employed the reaction worked at room temperature [70]. After a deep analysis of chemicals and conditions, we concluded that the impurities present on the commercially available BnN_3 were the responsible of the observed activity. GC-MS and NMR analyses proved that they consisted in amines bearing long alkyl chains. The addition of this kind of ligands to the reaction mixture, such as oleylamine, undecylamine, octylamine, dioctylamine or trioctylamine, led to the corresponding 1,4-triazole in nearly quantitative yields under smooth conditions. This behavior was also observed for other alkynes and azides, obtaining from moderate to high yields (Scheme 4).

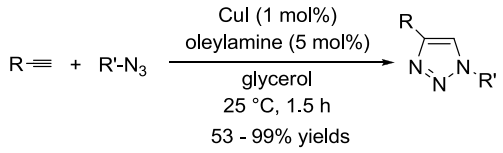

R' = Bn and R = Ph, CO_2Et, Cyp, $-CH_2-CH_2-Br$, $-CH_2-CH_2-OH$, $-CH_2-CH_2-CO_2Me$, n-Bu, $-CH_2-NMe_2$, $4-NO_2-C_6H_4$, $4-OMe-C_6H_4$

R' = Ph and R = Ph, n-Bu, $-CH_2-NMe_2$, $-CH_2-CH_2-Br$

Scheme 4. CuI/oleylamine catalytic system in glycerol for the synthesis of 1,4-triazoles [68].

The reason why the CuI/amine catalytic system is active lies in the *in situ* formation of Cu(I)-based nanocatalysts, as observed by (HR)TEM analyses (Figure 5), due to the stabilizing effect caused by the long chain amines [71]. The presence of short chain amines such as diisopropylethylamine or ethylenediamine, gave inactive CuI agglomerates.

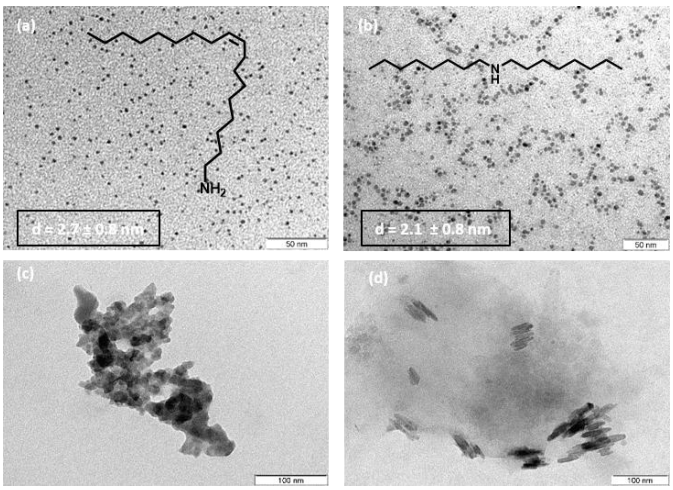

Figure 5. TEM images for CuI-based systems containing oleylamine (a), dioctylamine (b), ethylenediamine (c) and diisopropylamine (d) in glycerol. Reprinted with permission from reference [68]; license number 4040821133598. Copyright 2017, John Wiley and Sons.

4. Miscellaneous

Porous cube-aggregated monodisperse Co_3O_4 microspheres and their supported gold NPs (xAu/Co_3O_4 microsphere, x = 1.6–7.4 wt %) have been fabricated using the glycerol-assisted solvothermal and polyvinyl alcohol-protected reduction methods. These materials have been characterized by means of numerous analytical techniques and their catalytic behavior has been evaluated for the oxidation of carbon monoxide and toluene. Among the different samples, the $7.4Au/Co_3O_4$ microspheres performed the best. The authors concluded that the higher oxygen ad-species concentration, and stronger interaction between AuNPs and Co_3O_4 as well as the porous microspherical structure, were crucial parameters responsible for the excellent catalytic performance of $7.4Au/Co_3O_4$ microsphere [72].

Applications towards *p*-nitrophenol sensing have been recently described for ZnO microstructures. The fabrication of 3-dimensional flower-shaped ZnO microstructures from a zinc ammonium complex in the presence of glycerol encompasses the formation of zinc glycerolate, which in turn acts as suitable solvent to control the final morphology of the ZnO microstructure [73] (Figure 6).

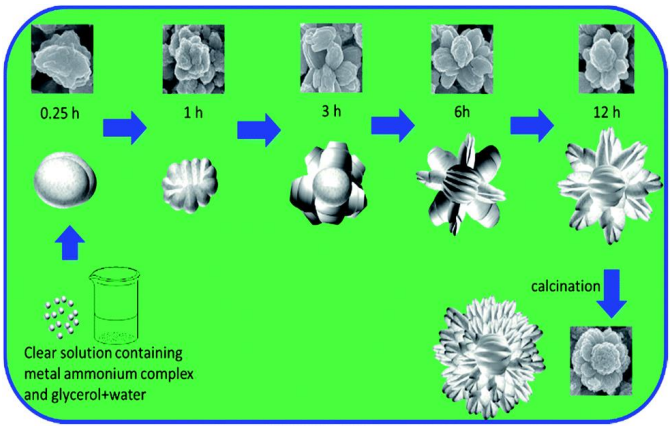

Figure 6. Schematic representation for stepwise formation of flower-shaped zinc glycerolate and corresponding ZnO microstructure. Reprinted with permission from reference [73]; license number 4040100302835. Copyright 2017, Royal Society of Chemistry.

A glassy carbon electrode can then be modified with this novel material providing an excellent binder-free non-enzymatic amperometric chemical sensor for the detection of *p*-nitrophenol pollutant with high sensitivity, selectivity and stability [73] (Figure 7).

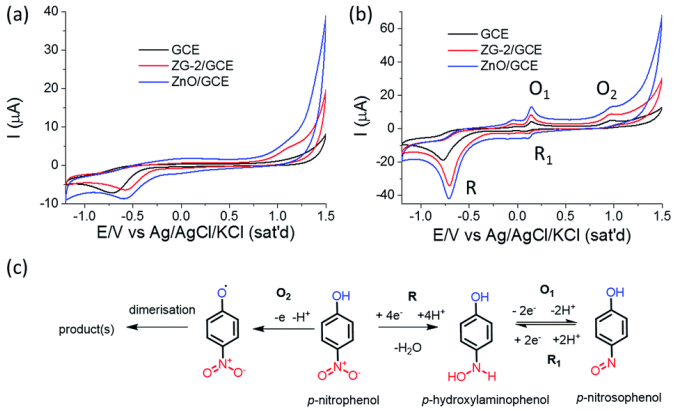

Figure 7. Cyclic voltammogram traces of bare glassy carbon electrode (GCE) and modified GCEs (a) in the absence and (b) in the presence of 0.5 mM of *p*-nitrophenol in phosphate buffered saline (pH 7) at a scan rate of 50 mV s−1. (c) Probable electrochemical redox reactions involved for *p*-nitrophenol sensing. Reprinted with permission from reference [73]; license number 4040100302835. Copyright 2017, Royal Society of Chemistry.

The hydrogen bonding, viscosity, and polarity properties of solvents play crucial effects towards the dispersion of nanoparticles in a liquid phase. A thorough study has been carried out by W. Chi et al. to assess the thermal conductivity of nanofluids containing Fe_2O_3 nanoparticles in different media. Despite the dramatic increase in viscosity for fluids with multiple OH groups, such as glycerol and ethylene glycol which plays a detrimental role towards dispersion and alignment of Fe_2O_3 NPs, mixtures of polyol-water (50:50) displayed significantly reduced viscosity and provided convenient particles dispersion and alignment with optimal thermal conductivity properties, since high thermal conductivity enhancement with minimal viscosity increase is the primary goal of heat transfer nanofluids [74].

Besides, the preparation of ZrO_2 nanomaterials by a sol-gel process with carbon as a phase transformation promoter has been discussed. Cubic and tetragonal ZrO_2 were synthesized from $ZrOCl_2 \cdot 8H_2O$ as zirconium source by a sol-gel method using ethanol and glycerol and characterized by powder X-ray diffraction (XRD), X-ray photoelectron spectroscopy (XPS), and scanning electron microscopy (SEM) [75].

Thus far, C. Daiguebonne, O. Guillou et al. have demonstrated that micrometric beads of lanthanide-based coordination polymers can be divided into nanometric particles via solvation of the lanthanide ions by glycerol. This process brings forth reliable means of synthesizing kinetically stabilized colloidal solutions of nanoparticles with both tunable luminescence properties and size. This approach brings forth new ways for the easy solubilization of lanthanide-based coordination polymers and enables the exploitation of the intrinsic luminescence properties of such compounds immobilized in liquid phase [76] (Figure 8).

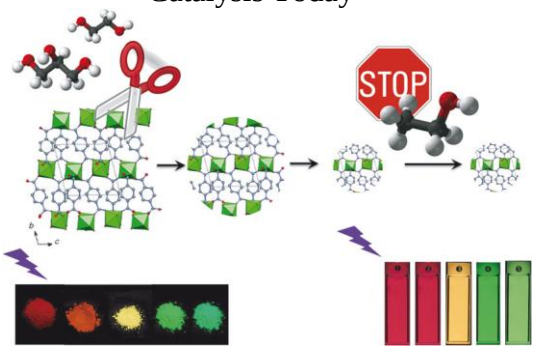

Figure 8. Lanthanide- based nanometric coordination polymers. Reprinted with permission from reference [76]; license number 4040121144382. Copyright 2017, John Wiley and Sons.

Thorium oxide nanoparticles were synthesized by hydrothermal method. It was found that glycerol acts as a size-controlling agent. The synthesis consists in the reaction between $Th(NO_3)_4 \cdot 5H_2O$, urea and glycerol. In the absence of glycerol, only heterogeneous mixtures were obtained. The addition of glycerol serves to fine-tune the size of the homogeneous precursor due to the coordination of glycerol to Th(IV) species in solution. When a moderate volume of glycerol is added, the number of nuclei decreases, and the growth step becomes slower. Pure ThO_2 NPs were obtained after calcination at 800 °C for 5 h under air [77].

5. Outlook and Perspectives

The novel methodologies described in the recent literature reports open up new opportunities towards the preparation of nanoparticles with optimal surface area and high selectivity to exploit the full potential of these novel materials as nanocatalysts in liquid phase. The enhanced immobilization properties of glycerol concerning metal species enables the implementation of flow chemistry technologies, as well as adsorption of glycerol catalytic phases on nano-structured materials including polymeric catalytic membranes. Furthermore, solvent engineering through chemical modifications may preclude the intrinsic reactivity of hydroxyl groups of glycerol, allowing the preparation of upgraded next generation solvents with optimal physical properties towards sustainable applications in catalysis. These tunable nanostructured materials shall provide excellent means towards both fundamental reactivity understanding of nano-systems, and synthetic applications under green chemistry premises. The virtually limitless possibilities associated to these new generation materials confer a huge potential towards innovative industrial methodologies given their recyclability and catalyst immobilization capabilities.

Acknowledgments

The Centre National de la Recherche Scientifique (CNRS), and the Université de Toulouse 3 – Paul Sabatier are gratefully acknowledged for their financial support.

References and notes

[1] Y. Gu, F. Jerome, Green Chem., 12 (2010) 1127-1138.
[2] A.E. Diaz-Alvarez, J. Francos, B. Lastra-Barreira, P. Crochet, V. Cadierno, Chem. Commun., 47 (2011) 6208-6227.
[3] F. Chahdoura, I. Favier, M. Gomez, Chem. Eur. J., 20 (2014) 10884-10893.
[4] P. Cintas, S. Tagliapietra, E. Calcio Gaudino, G. Palmisano, G. Cravotto, Green Chem., 16 (2014) 1056-1065.
[5] C. Gabriel, S. Gabriel, E. H. Grant, B. S. J. Halstead, D. Michael P. Mingos, Chem. Soc. Rev., 27 (1998) 213-224.

[6] F. Fievet, J.P. Lagier, B. Blin, B. Beaudoin, M. Figlarz, Solid State Ion., 32/33 (1989) 198-205.
[7] T.-H. Tran, T.-D. Nguyen, Colloids Surf B Biointerfaces, 88 (2011) 1-22.
[8] A.J. Biacchi, R.E. Schaak, ACS Nano, 5 (2011) 8089-8099.
[9] F. Chahdoura, C. Pradel, M. Gómez, Adv. Synth. Catal., 355 (2013) 3648-3660.
[10] M.A. Dasari, P.-P. Kiatsimkul, W.R. Sutterlin, G.J. Suppes, Appl. Catal., A, 281 (2005) 225-231.
[11] T. Kusukawa, G. Niwa, T. Sasaki, R. Oosawa, W. Himeno, M. Kato, Bull. Chem. Soc. Jpn., 86 (2013) 351-353.
[12] M. Kim, W.-S. Son, K.H. Ahn, D.S. Kim, H.-s. Lee, Y.-W. Lee, J. Supercrit. Fluids, 90 (2014) 53-59.
[13] C. Ding, J. Wang, G. Ai, S. Liu, P. Liu, K. Zhang, Y. Han, X. Ma, Fuel, 175 (2016) 1-12.
[14] M. Kapkowski, T. Siudyga, R. Sitko, J. Lelatko, J. Szade, K. Balin, J. Klimontko, P. Bartczak, J. Polanski, PLoS One, 10 (2015) e0142668/1-e0142668/15.
[15] T.B. Celic, M. Grilc, B. Likozar, N.N. Tusar, ChemSusChem, 8 (2015) 1703-1710.
[16] X. Yu, E.J. Pascual, J.C. Wauson, A. Manthiram, J. Power Sources, 331 (2016) 340-347.
[17] Y. Gao, D. Chen, M. Saccoccio, Z. Lu, F. Ciucci, Nano Energy, 27 (2016) 499-508.
[18] M. Harada, C. Cong, Ind. Eng. Chem. Res., 55 (2016) 5634-5643.
[19] M. Miyakawa, N. Hiyoshi, M. Nishioka, H. Koda, K. Sato, A. Miyazawa, T.M. Suzuki, Nanoscale, 6 (2014) 8720-8725.
[20] M. Rodríguez-Rodríguez, E. Gras, M.A. Pericàs, M. Gómez, Chem. Eur. J., 21 (2015) 18706-18710.
[21] K. Philippot, B. Chaudret, C. R. Chim., 6 (2003) 1019-1034.
[22] I. Favier, E. Teuma, M. Gómez, C. R. Chim., 12 (2009) 533-545.
[23] C. Amiens, D. Ciuculescu-Pradines, K. Philippot, Coord. Chem. Rev., 308, Part 2 (2016) 409-432.
[24] F. Chahdoura, I. Favier, E. Teuma, M. Gomez, Metal nano-catalysts in glycerol and applications in organic synthesis, PCT Int. Appl. (2014), WO 2014096732 A1 20140626; Fr. Demande (2014), FR 2999956 A1 20140627.
[25] F. Chahdoura, S. Mallet-Ladeira, M. Gomez, Org. Chem. Front., 2 (2015) 312-318.
[26] F. Chahdoura, I. Favier, C. Pradel, S. Mallet-Ladeira, M. Gómez, Catal. Commun., 63 (2015) 47-51.
[27] A. Reina, C. Pradel, E. Martin, E. Teuma, M. Gomez, RSC Adv., 6 (2016) 93205-93216.
[28] P.J. Collier, J.A. Iggo, R. Whyman, J. Mol. Catal. A: Chem., 146 (1999) 149-157.
[29] E. Schmidt, W. Kleist, F. Krumeich, T. Mallat, A. Baiker, Chem. Eur. J., 16 (2010) 2181-2192.
[30] F. Kirby, C. Moreno-Marrodan, Z. Baán, B.F. Bleeker, P. Barbaro, P.H. Berben, P.T. Witte, ChemCatChem, 6 (2014) 2904-2909.
[31] T.S.B. Trung, Y. Kim, S. Kang, S. Kim, H. Lee, Appl. Catal., A., 505 (2015) 319-325.
[32] D. Ferri, T. Bürgi, J. Am. Chem. Soc., 123 (2001) 12074-12084.
[33] A. Kraynov, A. Suchopar, L. D'Souza, R. Richards, Phys. Chem. Chem. Phys., 8 (2006) 1321-1328.
[34] A. Vargas, A. Baiker, J. Catal., 239 (2006) 220-226.
[35] R. Kannan, A.R. Kim, D.J. Yoo, J. Appl. Electrochem., 44 (2014) 893-902.
[36] Z.H.N. Al-Azri, W.-T. Chen, A. Chan, V. Jovic, T. Ina, H. Idriss, G.I.N. Waterhouse, J. Catal., 329 (2015) 355-367.
[37] V. Montes, M. Checa, A. Marinas, M. Boutonnet, J.M. Marinas, F.J. Urbano, S. Jaras, C. Pinel, Catal. Today, 223 (2014) 129-137.
[38] Y. Chen, M. Bellini, M. Bevilacqua, P. Fornasiero, A. Lavacchi, H.A. Miller, L. Wang, F. Vizza, ChemSusChem, 8 (2015) 524-33.
[39] X. Li, A.K. Tjiptoputro, J. Ding, J.M. Xue, Y. Zhu, Catal. Today, 279 (2017) 77-83.
[40] Z. Zhao, J.T. Miller, T. Wu, N.M. Schweitzer, M.S. Wong, Top. Catal., 58 (2015) 302-313.
[41] A. Villa, N. Dimitratos, C.E. Chan-Thaw, C. Hammond, L. Prati, G.J. Hutchings, Acc. Chem. Res., 48 (2015) 1403-1412.
[42] H.A. Miller, M. Bellini, F. Vizza, C. Hasenohrl, R.D. Tilley, Catal. Sci. Technol., 6 (2016) 6870-6878.
[43] R. Su, R. Tiruvalam, A.J. Logsdail, Q. He, C.A. Downing, M.T. Jensen, N. Dimitratos, L. Kesavan, P.P. Wells, R. Bechstein, H.H. Jensen, S. Wendt, C.R.A. Catlow, C.J. Kiely, G.J. Hutchings, F. Besenbacher, ACS Nano, 8 (2014) 3490-3497.
[44] L. Niu, Q. Zhang, S. Chao, M. Shi, R. Huang, Z. Bai, L. Yang, Ionics, 21 (2015) 1989-1996.
[45] A. Herbst, C. Janiak, CrystEngComm, (2016) DOI: 10.1039/C6CE01782G.
[46] G.K. Inwati, Y. Rao, M. Singh, Nanoscale Res. Lett., 11 (2016) 1-8.
[47] Z. Wang, Q. Suo, C. Zhang, Z. Chai, X. Wang, RSC Adv., 6 (2016) 89098-89102.
[48] K. Dobrovolný, P. Ulbrich, M. Švecová, V. Bartůněk, Metall. Mater. Trans. B, 46 (2015) 2529-2533.
[49] A.A. Antipov, S.M. Arakelian, D.N. Bukharov, T.E. Itina, S.V. Kutrovskaya, A.O. Kucherik, D.S. Nogtev, Bull. Russ. Acad. Sci. Phys., 80 (2016) 351-357.
[50] C. An, J. Wang, W. Jiang, M. Zhang, X. Ming, S. Wang, Q. Zhang, Nanoscale, 4 (2012) 5646-5650.
[51] H.R. Ong, M.M. Rahman Khan, R. Ramli, Y. Du, S. Xi, R.M. Yunus, RSC Adv., 5 (2015) 24544-24549.
[52] Q. Zhang, N. Li, J. Goebl, Z. Lu, Y. Yin, J. Am. Chem. Soc., 133 (2011) 18931-18939.
[53] D. Steinigeweg, S. Schlucker, Chem. Commun., 48 (2012) 8682-8684.
[54] P. Nalawade, P. Mukherjee, S. Kapoor, J. Nanostruct. Chem., 4 (2014) 113/1-113/8.
[55] A. Tadjarodi, F. Zabihi, Mater. Res. Bull., 48 (2013) 4150-4156.
[56] F. Chahdoura, C. Pradel, M. Gómez, ChemCatChem, 6 (2014) 2929-2936.
[57] H. Xu, C. Wolf, Chem. Commun., (2009) 3035-3037.
[58] Z. Quan, H. Xia, Z. Zhang, Y. Da, X. Wang, Chin. J. Chem., 31 (2013) 501-506.
[59] V.V. Rostovtsev, L.G. Green, V.V. Fokin, K.B. Sharpless, Angew. Chem. Int. Ed., 41 (2002) 2596-2599.
[60] C.W. Tornøe, C. Christensen, M. Meldal, J. Org. Chem., 67 (2002) 3057-3064.
[61] J.E. Hein, V.V. Fokin, Chem. Soc. Rev., 39 (2010) 1302-1315.
[62] S. Díez-González, Catal. Sci. Technol., 1 (2011) 166-178.
[63] F. Alonso, Y. Moglie, G. Radivoy, Acc. Chem. Res., 48 (2015) 2516-2528.
[64] E. Haldon, M.C. Nicasio, P.J. Pérez, Org. Biomol. Chem., 13 (2015) 9528-9550.
[65] S. Chassaing, V. Beneteau, P. Pale, Catal. Sci. Tech., 6 (2016) 923-957.
[66] P. Etayo, C. Ayats, M.A. Pericàs, Chem. Commun., 52 (2016) 1997-2010.
[67] H.C. Kolb, M.G. Finn, K.B. Sharpless, Angew. Chem. Int. Ed., 40 (2001) 2004-2021.
[68] M. Rodríguez-Rodríguez, P. Llanes, C. Pradel, M.A. Pericàs, M. Gómez, Chem. Eur. J., 22 (2016) 18247-18253.
[69] S.G. Alvarez, M.T. Alvarez, Synthesis, 1997 (1997) 413-414.
[70] C. Vidal, J. García-Alvarez, Green Chem., 16 (2014) 3515-3521.
[71] M.R. Axet, K. Philippot, B. Chaudret, M. Cabié, S. Giorgio, C.R. Henry, Small, 7 (2011) 235-241.

[72] H. Yang, H. Dai, J. Deng, S. Xie, W. Han, W. Tan, Y. Jiang, C.T. Au, ChemSusChem, 7 (2014) 1745-1754.
[73] A. Sinhamahapatra, D. Bhattacharjya, J.-S. Yu, RSC Advances, 5 (2015) 37721-37728.
[74] G. Christensen, H. Younes, H. Hong, P. Smith, J. Appl. Phys., 118 (2015) 214302/1-214302/9.
[75] Y. Liu, W. Chi, H. Liu, Y. Su, L. Zhao, RSC Advances, 5 (2015) 34451-34455.
[76] C. Neaime, C. Daiguebonne, G. Calvez, S. Freslon, K. Bernot, F. Grasset, S. Cordier, O. Guillou, Chem. Eur. J., 21 (2015) 17466-17473.
[77] L. Wang, R. Zhao, X.-w. Wang, L. Mei, L.-y. Yuan, S.-a. Wang, Z.-f. Chai, W.-q. Shi, CrystEngComm, 16 (2014) 10469-10475.